SLOPE-FAN DEPOSITIONAL ARCHITECTURE FROM HIGH-RESOLUTION FORWARD STRATIGRAPHIC MODELS

Nicolas Hawie[1], **Jacob A. Covault**[2], **Dallas Dunlap**[2], **and Zoltán Sylvester**[2]

[1]*Beicip Franlab, Rueil-Malmaison, France*

[2]*Bureau of Economic Geology, Jackson School of Geoscience, The University of Texas at Austin, Austin, TX, USA*

ABSTRACT

Submarine fans in tectonically active continental-slope basins are targets of petroleum exploration and production. These slope fans commonly comprise compensationally stacked sandy and muddy architectural elements, including mass-transport deposits, weakly confined to distributary channel-and-lobe deposits, and leveed-channel deposits. The lateral continuity and vertical connectivity of these architectural elements are important uncertainties in reservoir characterization that influence fluid-flow behavior during hydrocarbon production. Here, we use a simple forward stratigraphic model to reproduce the large-scale stratigraphic patterns and illuminate the likely distribution of finer-scale, sub-seismic heterogeneity in a slope fan. We used three-dimensional seismic-reflection data (~40 Hz dominant frequency) in the tectonically active Columbus basin, offshore Trinidad, to document the Pleistocene stratigraphic architecture and evolution of a submarine fan across a stepped slope profile. Isochron maps of the fan show a pattern of compensational stacking of deposits; we interpret that sediment-gravity flows avoided pre-existing mass-transport-deposit topography, and formed compensationally stacked channel-and-lobe deposits. Once the stepped slope profile was healed by deposition, a leveed channel promoted bypass of sediment beyond the study area. We then evaluated our interpretation of compensation with a series of DionisosFlow™ forward stratigraphic models. All variables were kept constant during the simulations in order to test the hypothesis that the autogenic evolution of the surface topography alone, as a result of erosion and deposition, can produce the compensational-stacking patterns interpreted in the seismic-reflection data. A reference-case model generally matches the thickness trend of our seismic-stratigraphic interpretation; it also produced similar large-scale patterns of compensational stacking and depocenter evolution. However, varying the time step impacts the heterogeneity of the model. Shorter time steps are characterized by less sediment accumulation, which results in less sediment diversion during the subsequent time step, more gradual migration of channel deposits, shorter offset distances of depocenters, and shorter length-scale heterogeneity compared to longer time steps. Thus, a key characteristic of slope-fan deposits is autogenic compensational stacking, without any external forcing, which governs heterogeneity in these reservoirs. Furthermore, our results suggest that relatively simple diffusion-based models can produce realistic compensation patterns.

INTRODUCTION

Submarine fans are depositional sinks of continental-margin sediment-routing systems, where they host stratigraphic archives of Earth history and environmental changes (Clift and Gaedicke, 2002; Fildani and Normark, 2004; Covault et al., 2010; 2011; Fildani et al., 2016). Submarine fans are also important reservoirs of natural resources (Pettingill and Weimer, 2002). Early models characterized submarine fans as laterally extensive sheets in cross section with radial- or cone-like depositional morphologies in map view across unconfined basin floors of low relief and with gentle gradients (e.g., Shepard and Emery, 1941; Dill et al., 1954; Menard, 1955; Heezen et al., 1959; Bouma et al., 1985) (Fig. 1). However, receiving-basin geometry and tectonic deformation can influence the organization of sandy and muddy architectural elements of submarine fans (Piper and Normark, 2001). For example, tectonically active slope basins and stepped slopes with abrupt changes in gradient commonly consist of ponded mass-transport deposits overlain by weakly confined to distributary channel-and-lobe deposits, which transition to perched, downstream-thinning wedges comprising leveed-channel deposits (Beaubouef and Friedmann, 2000; Brami et al., 2000; Beaubouef et al., 2003; Prather, 2003) (Fig. 1); although, mass-transport deposits and leveed channels are not always present (e.g., Jobe et al., 2017). Such tectonically active slopes are targets of petroleum exploration and production (e.g., the slope basins and stepped slopes of the Gulf of Mexico and the Niger Delta; Damuth, 1994; Pirmez et al., 2000; Sullivan et al., 2004a; Prather, 2003; Rowan et al., 2004; Adeogba et al., 2005; Deptuck et al., 2012; Sylvester et al., 2012).

Models of slope-fan stratigraphic architecture and evolution are predominantly based on insights from shallow-subsurface 3-D seismic-reflection data (up to ~200 Hz peak frequency), with limited core penetrations (e.g., Beaubouef and Friedmann, 2000; Beaubouef et al., 2003; Prather et al., 2012; Pirmez et al., 2012). These datasets can constrain the 3-D geometry of packages of strata as thin as several tens of meters in the subsurface, but they lack the depth of penetration and deep-time perspective of conventional industry seismic-reflection data (e.g., generally <40 Hz peak frequency; Normark et al., 1993; Prather et al., 2012). Moreover, core calibration is limited and does not provide a strong 3-D lithologic control, which can be of importance to the spatial variation in properties in oil and gas reservoirs (i.e., heterogeneity; Lake and Jensen, 1989). These datasets provide insights into the compensational stacking of architectural elements and the stratigraphic evolution from ponded to perched fan deposits. However, an important applied question is the lateral continuity and vertical connectivity of sandy and muddy architectural elements at higher resolution. These architectural elements control the static and dynamic connectivity of slope-fan reservoirs and influence fluid-flow behavior during hydrocarbon production (e.g., Glenton et al., 2013; Sutton et al., 2013).

Deptuck et al. (2008) used high-resolution 2-D seismic-reflection profiles (900-7000 Hz frequencies) and piston cores to investigate the causes of heterogeneity in Pleistocene submarine fans offshore East Corsica. This work provided new details of the hierarchical levels of compensational stacking of deposits: individual beds stack to form lobe architectural elements, which stack to form more composite submarine fans. However, the high-resolution 2-D imagery of the Pleistocene deposits offshore East Corsica lacks the 3-D perspective of fan geometry. Physical experiments provide high temporal- and spatial-resolution insights into the morphodynamic processes of sediment-gravity flows and fans (e.g., Spinewine et al., 2009; Hoyal et al., 2011; 2014; Fernandez et al., 2014; Hamilton et al., 2015; Postma et al., 2016); however, these studies lack the long-term (>10^3 yr) perspective of stratigraphic evolution and the complexity of field-scale depositional elements. Nevertheless, physical experiments offer the opportunity to constrain fundamental processes that operate in slope depositional environments when combined with other approaches, such as 3-D seismic-stratigraphic interpretation and forward stratigraphic modeling.

Forward stratigraphic modeling can provide insights into the long-term (>10^3 yr) stratigraphic evolution of slope fans at high temporal and spatial resolution (e.g., Miller et al., 2008; Sun et al., 2010). Here, we evaluate the efficacy of a simple forward stratigraphic model to reproduce the large-scale stratigraphic patterns and illuminate the finer-scale, sub-seismic heterogeneity of a slope fan. We used 3-D seismic-reflection data (~40 Hz dominant frequency) in the Columbus basin, offshore Trinidad, to document the Pleistocene stratigraphic architecture and evolution of a submarine fan in a tectonically active slope. We then evaluate our interpretation of stratigraphic patterns with a series of DionisosFlow^{TM} forward stratigraphic models (17 km x 17 km area; 200 m x 200 m grid size). All variables are kept constant during the simulations to test the hypothesis that the autogenic evolution of the surface topography alone, without any external forcing, can produce the compensational-stacking patterns of our seismic-stratigraphic interpretation. We test the sensitivity of the models to time step (20 kyr, 10 kyr, 5 kyr, and 1 kyr), and discuss the impact of varying the time step on the lateral continuity and vertical connectivity of sandy and muddy architectural elements in slope fans. These interpretations inform the prediction of 3-D sub-seismic heterogeneity of slope fans and demonstrate the value of integrated subsurface characterization and forward stratigraphic modeling to understand the range of reservoir connectivity and quality in such settings.

GEOLOGIC SETTING

Oblique subduction of the South American plate beneath the eastward migrating Caribbean plate since the Miocene promoted the development of the east-west-oriented Columbus foreland-basin system in the present-day shelf offshore of eastern Trinidad (Leonard, 1983; Wood, 2000; Weber et al., 2001; Huyghe et al., 2004; Garciacaro et al., 2011a; 2011b) (Fig. 2). The Columbus basin contains nearly 500 MMBBL of oil and >20 TCF of gas (Wood and Roberts, 2001). Transpression along the Central Range fault zone created a fold-thrust belt in Trinidad (Escalona and Mann, 2011). The offshore expression of the Central Range fault zone is the northwest-southeast-oriented Darien ridge, which defines the boundary between the Columbus basin and the Barbados accretionary wedge on the slope offshore of eastern Trinidad (Wood, 2000; Wood and Mize-Spansky, 2009; Moscardelli et al., 2012). The Darien ridge and related fold-thrust structures form highs on the present-day seafloor that locally exhibit >100 m of relief (Garciacaro et al., 2011a; 2011b; Moscardelli et al., 2012). Fold-thrust-belt deformation and tectono-sedimentary loading of Miocene-Pliocene sediment promoted mud diapirism and the development of northeast-southwest-oriented mud-volcano ridges on the seafloor (up to several hundreds of meters of relief) and shallow subsurface of the slope offshore of eastern Trinidad (Sullivan et al., 2004b; Garciacaro et al., 2011a; 2011b; Moscardelli et al., 2012). High-relief fold-thrust structures and mud volcanoes influence the pathways of down-slope sediment dispersal and the resulting stratigraphic architecture of mass-transport deposits and submarine canyon-channel-fan systems offshore of eastern Trinidad (Brami et al., 2000; Moscardelli et al., 2006; Wood and Mize-Spansky, 2009). Northwest-southeast-trending normal faults dominate the Columbus basin shelf and upper slope and accommodate local depocenters (Wood, 2000; Moscardelli et al., 2006).

The Orinoco river-delta system has delivered terrigenous sediment to the Columbus basin and continental margin offshore of Trinidad since the Miocene (>12 km of Pliocene-Pleistocene stratigraphic thickness; Leonard, 1983; de Gamero, 1996; Wood, 2000). The Orinoco river drains the third largest catchment (>10^6 km^2) and delivers the second largest suspended-sediment load (>200 Mt/yr) to the ocean in South America (Milliman and Farnsworth, 2011). Sediment delivery from the Orinoco river promoted the development of some of the northwest-southeast-trending normal faults in the shelf and upper slope (Wood, 2000; Moscardelli et al., 2006; Garciacaro et al., 2011b), as well as mud diapirism across the margin (Sullivan et al., 2004b). During the last glacial maximum (~20 ka), the Orinoco delta was located at the shelf edge, ~100 km east of present-day Trinidad, and delivered terrigenous sediment directly into canyon-channel systems on the slope east of the Columbus basin (Sydow et al., 2003; Moscardelli et al., 2006; Moscardelli, 2007). Since then, 125 m of eustatic rise resulted in transgression of the shoreline and retrogradation of the delta to its present-day position on the coast of eastern Venezuela (Warme et al., 2002). Terrigenous sediment from the Orinoco river-delta system is transported from west to east by sediment-gravity flows across the tectonically active slope to the toe of the Barbados accretionary wedge and the Atlantic abyssal plain (Belderson et al., 1984; Faugeres et al., 1993; Huyghe et al., 2004).

The focus area of this study is located on the tectonically active slope east of the Columbus basin and along the southern margin of the Barbados accretionary wedge (the 'NW' depocenter between the Darien and Haydn ridges in block 25A offshore of Trinidad; Brami et al., 2000; Wood and Mize-Spansky, 2009) (Figs. 2 and 3). We modeled the late Pleistocene stratigraphic architecture and evolution of a slope fan beyond a break in slope at ~1000 m water depth (Figs. 3 and 4). Brami et al. (2000) interpreted the late Pleistocene seismic-stratigraphic evolution of stacked channel fills and associated levee-overbank deposits, mass-transport deposits, and mud volcanoes, among other, less prominent, architectural elements of the margin. The orientations of leveed channels and their deposits were interpreted to be influenced by mud volcanoes and the surface topography of mass-transport deposits (cf. Armitage et al., 2009; Kneller et al., 2016). Moscardelli et al. (2006) interpreted the seismic-stratigraphic architecture of mass-transport deposits in the region comprising large-scale erosional margins, linear basal scours, and side-wall failures. Moscardelli and Wood (2008) classified the mass-transport deposits based on their sourcing regions, i.e., from failure of shelf-edge deltas or the open slope with run-out distances ranging from several km to >100 km. Wood and Mize-Spansky (2009) characterized the seafloor geomorphology and shallow-subsurface seismic stratigraphy of seven leveed channels in the region. Channel patterns were interpreted to be strongly influenced by topographic highs, including fold-thrust structures and mud volcanoes, across the tectonically active slope (Wood and Mize-Spansky, 2009). Exploration drilling in block 25A (Haydn-1 well) revealed a thick section

(>3 km) of Pliocene-Pleistocene slope-fan deposits (Patterson et al., 2001) (Fig. 2). We interpreted the shallow-subsurface seismic stratigraphy above the 'P20' regional horizon of Brami et al. (2000) (<200 ms TWTT below the seafloor), which is approximately the '2' horizon of Moscardelli et al. (2006), the 'P10' horizon of Moscardelli and Wood (2008), and the 'Pleist. 05' horizon of Garciacaro et al. (2011b).

DATA AND METHODS

Seismic-Stratigraphic Interpretation

We used published 3-D seismic-reflection data to interpret the stratigraphic evolution of a submarine fan on the tectonically active slope east of the Columbus basin in block 25A offshore of Trinidad (Fig. 3). The seismic-reflection volume in block 25A is part of a set of volumes spanning nearly 11,000 km^2 that has been published in peer-reviewed literature by the Quantitative Clastics Laboratory at the Bureau of Economic Geology, the University of Texas at Austin (e.g., Moscardelli et al., 2006; Moscardelli and Wood, 2008; Wood and Mize-Spansky, 2009; Garciacaro et al., 2011b) (Figs. 2 and 3). The seismic-reflection dataset is also the subject of unpublished MS theses at the University of Texas at Austin (e.g., Mize, 2004; Sullivan, 2005). Block 25A is covered by a time-migrated seismic-reflection volume (~1490 km^2) with 25 m x 25 m bin spacing and vertical samples every 4 ms TWTT (Garciacaro et al., 2011b). Seismic-reflection data were processed to zero phase, and the dominant frequency of the full-stack data in the shallow subsurface (<200 ms TWTT below the seafloor) is ~40 Hz. Peaks are black and troughs are white in Figure 4. Tuning thickness is ~12.5 m based on a frequency of 40 Hz and velocity of ~2000 m/s in the shallow subsurface.

We used the Paradigm® SeisEarth® interpretation and visualization product suite to map six regional horizons based on continuity and terminations of relatively high-amplitude seismic reflections (Fig. 4). Figure 5 shows isochron maps of five packages of concordant reflections bounded by the six regional horizons. We defined seismic facies and interpreted architectural elements within these packages on the basis of the amplitude, continuity, and configuration of reflections (Mitchum et al., 1977; Walker, 1992; Normark et al., 1993).

Forward Stratigraphic Modeling

DionisosFlow™ software is a four dimensional process-based deterministic multi-lithology forward stratigraphic model that simulates basin filling (Granjeon, 1997; Granjeon and Joseph, 1999; Granjeon, 2014). A range of sedimentary processes are modeled including diffusive sediment transport, delta autoretreat, incision, large-scale avulsion, and slope failure in response to tectonic, climate, and sea-level fluctuations during millennia and longer time scales (e.g., Pinheiro-Moreira, 2000; Rabineau et al., 2005; Alzaga-Ruiz et al., 2009; Gvirtzman et al., 2014; Harris et al., 2016; Hawie et al., 2017). Detailed fluid dynamics are not considered in this model; the goal is to simulate the large-scale (10^2-10^3 m cell size) and long-term (10^3-10^5 yr time steps) evolution of basin fill.

Sediment transport equations are used to simulate the transport of various classes of sediment grain size (e.g., clay and sand) across a basin. This stratigraphic model combines 1) linear slope-driven diffusion (transport proportional to slope), referred to as hillslope creep, and 2) non-linear water- and slope-driven diffusion, referred to as water-discharge-driven transport (Willgoose et al., 1991; Tucker and Slingerland, 1994; Granjeon, 1997; Granjeon and Joseph, 1999; Deville et al., 2015):

$$Q_s = -\left(K_s/\vec{\nabla}h + K_w Q_w^m S^n\right)$$

where Q_s is sediment flux (km^2/yr), K_s and K_w are the slope- and water-driven diffusion coefficients, respectively (km^2/yr), Q_w is the dimensionless water flux, n and m are exponents that affect sediment transport capacity with values between 1 and 2 (Tucker and Slingerland, 1994), S is the dimensionless local gradient of the basin, and h (m) is topographic elevation (Granjeon, 2014). Sedimentation and erosion rates are quantified by a mass balance equation in 3-D for each class of grain size (Euzen et al., 2004). Our goal was to simulate the large-scale (10^2 m cell size) and long-term (10^3-10^4 yr time steps) stratigraphic evolution of a submarine fan within a 17 km x 17 km area of a stepped slope offshore of Trinidad (Table 1). Sediment-gravity flows, commonly turbidity currents, are the primary agents of sediment transport, erosion, and deposition in submarine fans and related turbidite systems (Bouma et al., 1985). We liken the water-driven diffusion coefficient and the dimensionless water flux to a sediment-gravity-flow-driven diffusion coefficient and gravity-flow flux, respectively, which govern the rate of sediment transport though the system. We have tuned the variables of the diffusion equation, including the gravity-flow-driven diffusion coefficient and dimensionless gravity-flow flux, to achieve a result that was consistent with our seismic-stratigraphic interpretation in a reference-case model.

Model Framework

The goals of the modeling were to evaluate our seismic-stratigraphic interpretation of the slope fan: can the overall seismic-stratigraphic patterns be reproduced, including thickness trend and compensational stacking? We also aimed to assess the impact of duration of time step (20 kyr, 10 kyr, 5 kyr, and 1 kyr), flow properties, and seafloor topography on the size, shape, and sub-seismic stacking and heterogeneity of leveed-channel and lobe architectural elements of the fan.

Models calibrated to geological and geophysical data (e.g., seismic reflections) are referred to as "reference cases." We modeled a reference case for a late Pleistocene period during the last glacial cycle (124.5-24.5 ka) within a bounding box of 17 km x 17 km with cell sizes of 200 m x 200 m and an initial simulated time step of 10 kyr (Table 1). The down-dip model boundary was set as open in order to allow sediment transport outside of the model domain. Deville et al. (2015) recently used DionisosFlow™ to model large-scale sediment fairways and facies distribution of turbidite systems (1200 km x 1200 km area; 10 km x 10 km grid size). However, this is the first high-resolution DionisosFlow™ forward stratigraphic model of a slope fan with a 300-600 m-wide feeder channel at sub-seismic resolution, using grain sizes ranging from sand to clay. We used the regional surface at the base of the slope fan, horizon 'c,' which overlies mass-transport deposits mapped by Moscardelli et al. (2006), as the initial bathymetry of the model. The feeder channel is in the south based on the seismic-stratigraphic interpretations (Figs. 3-5).

We did not account for differential subsidence in the model. The transport parameters used for the reference case model range from 10 to 100 km^2/kyr for water-driven diffusion (or, in the case of submarine fans, sediment-gravity-flow-driven diffusion; K_w) and 0.001 to 0.1 km^2/kyr for slope-driven transport (K_s) (Table 1). We determined these ranges of diffusion coefficients based on simplifying the diffusion equation to $Q_s = K_w Q_w S$ and solving for K_w based on Q_s, Q_w, and S from the Trinidad slope-fan system. The slope-driven diffusion coefficient (K_s) is relatively small, several orders of magnitude less than the water-driven diffusion coefficient (K_w) (Flemings and Jordan, 1989; Avouac and Burov, 1996). For our depositional system, slope-driven diffusion has less impact on model results compared to the water-driven diffusion coefficient (K_w) because of very small gradients of the basin floor. These parameters are within the lower order of magnitude of Deville et al. (2015), who modeled a complete source-to-sink system. Ratios of diffusion coefficients are applied to different grain sizes (Table 1) (Granjeon, 1997; Granjeon and Joseph 1999; Euzen et al., 2004; Granjeon 2014). Reference-case model calibration is based on 1) thicknesses trends in isochron maps, 2) compensational stacking patterns and depocenter evolution, and 3) seismic facies and architectural elements. Following the reference-case model calibration, we varied the simulated time step (20 kyr, 5 kyr, and 1 kyr).

RESULTS

Seismic-Stratigraphic Interpretation

We mapped six regional horizons named, from stratigraphically old to young, ‘a,’ ‘b,’ ‘c,’ ‘d,’ ‘e,’ and the seafloor is ‘f’ (Fig. 4). In map view, horizons ‘a’ and ‘b’ exhibit extensive and irregular erosional characteristics (e.g., steep erosional edges >100 ms TWTT in relief, as well as linear grooves or scours in core regions) (Fig. 5); in cross section, horizons ‘a’ and ‘b’ define the bases of a pair of compensationally stacked wedge-shaped seismic-reflection packages composed of chaotic, discontinuous, low-amplitude seismic reflections (Figs. 4 and 5). We interpret the seismic-reflection packages immediately above horizons ‘a’ and ‘b’ to be mass-transport deposits at the base of the youngest depositional sequence in block 25A (cf. Moscardelli et al., 2006). Isochron maps between horizons ‘c’-‘d’ and ‘d’-‘e’ approximate fan-like geometries (Fig. 5); in cross section, the seismic-reflection packages between horizons ‘c’-‘d’ and ‘d’-‘e’ are lenticular and compensationally stacked, with discontinuous (~200-300 m wide), high-amplitude channel-form seismic reflections (Figs. 3b and 4). Some of the channel-form seismic reflections are bounded by semi-continuous (several km), single-cycle, high-amplitude seismic reflections (Fig. 4). The seismic-reflection packages thin downstream, to the north (Fig. 5). We interpret these seismic-reflection packages to be weakly confined channel-and-lobe deposits with local levee-overbank strata (Figs. 3b, 4, and 5). The discontinuous, high-amplitude channel-form seismic reflections represent weakly confined channel deposits; the more continuous high-amplitude seismic reflections represent lobe deposits and/or low-relief levee-overbank deposits bounding channels (cf. Brami et al., 2000) (Figs. 3b, 4, and 5).

Wood and Mize-Spansky (2009) interpreted leveed-channel deposits at the top of the depositional sequence, between horizon ‘e’ and the seafloor, horizon ‘f’ (i.e., ‘channel 1’ of Wood and Mize-Spansky, 2009) (Figs. 4 and 5). On the seafloor, the channel exhibits a concave-up cross section bounded by gullwing-shaped levee-overbank wedges (Brami et al., 2000; Wood and Mize-Spansky, 2009) (Fig. 4). Wood and Mize-Spansky (2009) reported >80% sand in a drop core collected from the thalweg of this channel (5 m penetration).

Isochron maps clearly show a pattern of compensational stacking of deposits reflecting an overall evolution from early mass-transport deposition to later weakly confined channel-and-lobe deposition, and culminating with levee-confined channel deposition (Brami et al., 2000; Wood and Mize-Spansky, 2009) (Fig. 5). We document three large-scale shifts of depocenters above the mass-transport deposits and between horizons ‘c’-‘f’: initially, the depocenter between horizons ‘c’-‘d’ was oriented southwest-to-northeast; then, between horizons horizons ‘d’-‘e,’ it was oriented more south-to-north; and, finally, between horizons ‘e’-‘f,’ it was oriented southwest-to-northeast again (Fig. 5). These phases of sediment diversion reflect compensational stacking in response to the construction of depositional topography of the order of 10^1 ms TWTT. The low resolution of the 3-D seismic-reflection data in block 25A challenges us to unequivocally interpret the individual channel-and-lobe architectural elements of the slope fan, especially between horizons ‘c’-‘d’ and ‘d’-‘e’; individual channel-and-lobe architectural elements can be thinner than the tuning thickness of the seismic-reflection data (for dimensions of channel and lobe architectural elements see Prélat et al., 2010; and McHargue et al., 2011). We evaluate our interpretation of large-scale compensational stacking with a series of forward stratigraphic models, which also provide insights into the sub-seismic hierarchical structure of slope fans.

Forward Stratigraphic Modeling

Our reference-case model (10 kyr time steps) reproduced the large-scale seismic-stratigraphic patterns of the slope fan in block 25A offshore of Trinidad (compare Figs. 5 and 6; Supplementary Files 1 and 2). We also tested the influence of varying the simulated time step (20 kyr, 5 kyr, and 1 kyr) on the sub-seismic heterogeneity of the slope fan, including the geometries of sandy and muddy architectural elements (Fig. 7; Supplementary Files 3-8). We kept all variables constant during the simulations to evaluate the hypothesis that the evolution of the surface topography alone, as a result of erosion and deposition independent of any external forcing, can produce the compensational-stacking patterns observed in the seismic-reflection data.

For the reference case, following the seismic-stratigraphic interpretation presented above (Brami et al., 2000; Moscardelli et al., 2006; Wood and Mize-Spansky, 2009), a 300-600 m-wide feeder channel was positioned in the southwestern part of the model. Sediment was transported to the north along a gentle regional slope (<0.5°) and diverted around locally rugose topography of underlying mass-transport deposits and mud volcanoes. The model output shows at least four major phases of sediment diversion during the migration of a relatively coarse-grained depocenter. Initially, the depocenter was oriented southwest-to-northeast (0.124-0.084 Ma), then it shifted to the west and was oriented more south-to-north (0.084-0.064 Ma), then it split into two concomitant depocenters (0.064-0.034 Ma) and, finally, it returned to a southwest-to-northeast orientation

(0.034-0.024 Ma) (Fig. 6; Supplementary Files 1 and 2). These phases of sediment diversion reflect compensational stacking in response to the construction of depositional topography similar in scale to the seismic-reflection data in block 25A (Fig. 5). Moreover, the overall proximal-to-distal thickness trend of the model matches the isochron maps (Fig. 6), although the proximal part of the model is approximately two times thicker (Fig. 6c). This thickness difference is likely a result of the challenge of simulating significant sediment bypass with the limited processes used in this simplistic diffusion-based model. However, as stated above, a goal of this modeling was to evaluate whether the overall seismic-stratigraphic patterns can be reproduced, and the overall trends of thinning and compensational stacking are similar (Figs. 5 and 6). While the seismic-stratigraphic interpretation can provide insights into the general thickness trends in the subsurface, the reference-case forward stratigraphic model also shows plausible patterns of lateral and vertical distribution of grain sizes. A proximal-to-distal architectural trend is also apparent; the proximal reach of the model shows multiple compensationally stacked, relatively confined, coarse-grained leveed-channel deposits (several km wide), which transition distally to unconfined, finer-grained lobe deposits (~4 km wide) (Fig. 6f).

Varying the simulated time step (20 kyr, 5 kyr, and 1 kyr) resulted in a similar thickness trend and compensational stacking of depocenters as the reference-case model (Fig. 7; Supplementary Files 3-8). In particular, all models show three to four major phases of sediment diversion during the migration of a relatively coarse-grained depocenter (Fig. 7; Supplementary Files 3-8). Moreover, the overall proximal-to-distal trend from relatively coarse-grained leveed-channel to finer-grained lobe deposits is similar in all models (Fig. 7). However, the detailed 3-D heterogeneity varies between models. In the 20 kyr time-step model, ~4-5 discrete packages of proximal leveed-channel deposits are several km wide and expand and thin downstream to >5 km-wide distal lobe deposits (Fig. 7a). Grain size is consistent over several hundreds of m to several km. The vertical resolution of the model is lower than the reference-case model (of the order of 10^1 m-thick accumulations of sediment per time step). This is because sediment supply was kept constant in all simulations; therefore, longer time steps will produce thicker accumulations of sediment per time step. In the 5 kyr time-step model, more numerous (as many as 8-10) packages of leveed-channel deposits are ~2 km wide and expand and thin downstream to <4 km-wide distal lobe deposits (Fig. 7b). Grain size is consistent over several hundreds of m to approximately a km. The vertical resolution of the model is high, with accumulations of sediment per time step of the order of 10^0 m, which provides finer-scale perspectives of more frequent compensational stacking and the 3-D interstratification of sand and clay in distal lobe deposits. In the 1 kyr time-step model, >15 packages of leveed-channel deposits are ~1-2 km wide and expand and thin downstream to 2-4 km wide distal lobe deposits (Fig. 7c). Grain size varies rapidly over several hundreds of m and the vertical resolution of the model is high (of the orders of 10^{-1}-10^0 m-thick accumulations of sediment per time step). In this 1 kyr time-step model, the 3-D heterogeneity is at a resolution observed in outcropping submarine fans (e.g., Mutti and Normark, 1987; Sullivan et al., 2000; 2004a; Prélat et al., 2009).

Even though all models show similar patterns of compensational stacking, from a qualitative perspective, shorter time steps result more gradual migration of channel deposits, shorter offset distances of depocenters, and shorter length-scale heterogeneity compared to longer time steps. This is because less sediment accumulates during shorter time steps and, as a result, less sediment diversion during the subsequent time step is expected as the relatively coarse-grained depocenter migrates around the model domain. In contrast, more sediment accumulates during longer time steps, resulting in a thicker deposit, which generates steeper gradients and longer offset distances of depocenters. Thus, the controls on the compensational stacking and depocenter evolution are autogenic in these models.

DISCUSSION

Slope-Fan Depositional Model

Isochron maps of a depositional sequence across a tectonically active, stepped slope profile offshore of Trinidad show a pattern of compensational stacking of channel-and-lobe deposits (Figs. 3b, 4, and 5). Once the stepped slope profile was healed by deposition, the leveed channel expressed on the present-day seafloor promoted bypass of gravity flows beyond the study area. We used DionisosFlow™ to simulate the stratigraphic evolution of this slope fan. We kept all variables constant during the simulations in order to evaluate the hypothesis that the autogenic evolution of the surface topography alone, without any external forcing, can produce the compensational-stacking patterns observed in the seismic-reflection data. Our reference-case forward stratigraphic model generally matches the thickness trend of our seismic-stratigraphic interpretation; it also produced similar large-scale patterns of compensational stacking and depocenter evolution. However, varying time step impacts the heterogeneity of the model: shorter time steps result in more gradual migration of channel deposits, shorter offset distances of depocenters, and shorter length-scale heterogeneity compared to longer time steps (Fig. 7).

The stratigraphic evolution of the depositional sequence offshore of Trinidad is similar to other systems in tectonically active slopes (e.g., the Gulf of Mexico and the Niger Delta; Beaubouef and Friedmann, 2000; Beaubouef et al., 2003; Prather, 2003; Adeogba et al., 2005; Deptuck et al., 2012); sinuous leveed channels descend a high-gradient upper slope, encounter a slope break, and transition to compensationally stacked mass-transport deposits overlain by weakly confined channel-and-lobe and leveed-channel deposits (Brami et al., 2000; Moscardelli et al., 2006; Wood and Mize-Spansky, 2009) (Fig. 1). The sub-seismic-scale stratigraphic architecture of the channel-and-lobe deposits of the slope fan offshore of Trinidad reflects stacking and depositional processes simulated in other forward stratigraphic models, such as repeated cycles of channel avulsion, compensational stacking, and unconfined deposition at the mouths of channels (e.g., Sun et al., 2010). Compensational stacking is a key characteristic of submarine lobe deposits (e.g., Deptuck et al., 2008; Jobe et al., 2017), and our results suggest that relatively simple diffusion-based models can produce realistic compensation patterns. We interpret that the depositional sequence in block 25A offshore of Trinidad is representative of a globally significant class of submarine fans in tectonically active slope basins and stepped slopes with abrupt changes in gradient (e.g., Beaubouef and Friedmann, 2000; Sullivan et al., 2004a; Beaubouef et al., 2003; Prather, 2003; Adeogba et al., 2005; Deptuck et al., 2012; Sylvester et al., 2012; Hoyal et al., 2011; 2014).

Our suite of forward stratigraphic models generally matches the geometries of our seismic-stratigraphic interpretation as a result of the evolution of the surface topography alone, without the influence of other variables of the diffusion equation or changing boundary conditions, such as eustasy or subsidence. A difference between the model output and seismic-reflection data is that thicknesses in the proximal area of the model exceed thicknesses observed in the field (Fig. 6c). This difference is likely a result of the challenge to reproduce significant sediment bypass with the limited processes used in this simplistic diffusion-based model. However, the overall trend of thinning and the compensational stacking are similar. A remaining question is whether varying other input variables can produce a similar thickness trend to the seismic-reflection interpretations while preserving patterns of compensational stacking. Future work will focus on the influence of input variables, such as erosion rates, sediment load, dimensionless sediment-gravity-flow flux, and sediment grain-size proportion, as well as changing boundary conditions, such as tectonics and climate (e.g., Richards et al., 1998; Sømme et al., 2009; Hawie et al., 2017; Harris et al., 2016). Furthermore, future work could also compare the lithologic predictions of DionisosFlow™ to seismic attributes.

Application to Reservoir Characterization and Modeling

Models of slope-fan deposition from 3-D seismic-reflection data constrain the large-scale geometries of packages of strata in the subsurface; however, an important applied question is the lateral continuity and vertical connectivity of sandy and muddy architectural elements at higher resolution. These architectural elements control the static connectivity of submarine-fan reservoirs and influence fluid-flow behavior during hydrocarbon production (e.g., Glenton et al., 2013; Sutton et al., 2013). Offshore of Trinidad, the low resolution of the 3-D seismic-reflection data in block 25A challenges us to interpret sub-seismic heterogeneity of the slope fan. Forward stratigraphic modeling provides insights into the long-term (>10^3 yr) stratigraphic evolution of slope fans at high temporal and spatial resolution. In particular, the modeling provides insights into the plausible distribution of grain sizes within the slope fan.

Commonly used geostatistical methods in reservoir modeling use semivariograms, geometric parameters, and/or training images to reproduce spatial statistics from available conditioning data (e.g., seismic-reflection and well) and analogs, with limited use of insights from depositional processes or stratigraphic evolution (Pyrcz and Deutsch, 2014). However, in sedimentary systems, the complex interactions of topography and flow result in erosion and deposition that govern the lateral continuity and vertical connectivity of sandy and muddy architectural elements of submarine fans (Piper and Normark, 2001). Models that fail to account for these processes might not capture realistic heterogeneity of deposits (Miller et al., 2008; Pyrcz et al., 2015).

Reservoir models based on integration of subsurface data (e.g., seismic-reflection, wireline-log, and core) and outcrop analogs have been shown to effectively represent heterogeneity of submarine fans. For example, Sullivan et al. (2004a) produced an object-based model (Pyrcz et al., 2015) of the A-50 reservoir of the Diana field, Gulf of Mexico deep-water slope, as proximal-to-distal channelized-to-sheet-like and layered deposits based on insights from deep-water outcrop analog data (Fig. 8c). The fundamental objects in this reservoir model were channel deposits; a large number (>100) of these objects were initially inserted at the well locations and then inserted stochastically into interwell regions until volume (presumably net sand-to-gross stratigraphic thickness, or net-to-gross) targets were met. Figure 8 shows a net-to-gross map of the final model of Sullivan et al. (2004a), which resembles the distribution of sand in a section of similar thickness (~40 m maximum thickness) in our reference-case forward stratigraphic model (0.074-0.064 Ma; Fig. 8). Although the models in Figure 8 look similar, they are constructed in different ways: many conventional reservoir models are populated with a large number of channel-deposit objects so that a net-to-gross target is met, but these objects are placed without proper stratigraphic ordering and almost always without compensational stacking, whereas a diffusion-based forward stratigraphic model has proper stratigraphic ordering and realistic compensational stacking. We have shown that a relatively simple forward stratigraphic model is able to reproduce large-scale stratigraphic patterns of a submarine fan deposited across a tectonically active stepped slope. Future applied work on reservoir characterization and modeling should determine the rates of change in facies and net-to-gross within individual channel-and-lobe deposits and evaluate the impacts of sedimentologic and stratigraphic characteristics on fluid flow behavior during hydrocarbon production; particularly the 3-D stacking of architectural elements at various hierarchical scales (i.e., from individual beds to sandy and muddy architectural elements to larger-scale depocenters interpreted in seismic-reflection data; Deptuck et al., 2008) and different scales of heterogeneity depending on model time step.

CONCLUSION

We combined 3-D seismic-stratigraphic interpretation and forward stratigraphic modeling to constrain fundamental processes that operate in slope fans. Sediment-gravity flows avoided pre-existing mass-transport-deposit topography and formed compensationally stacked channel-and-lobe deposits. Once the slope profile was healed by deposition, a leveed channel promoted bypass of sediment to deeper water. We used a simple forward stratigraphic model to reproduce stratigraphic patterns, including thickness trend and compensational stacking, and illuminate the likely distribution of finer-scale, sub-seismic heterogeneity in the slope fan. The evolution of the surface topography, as a result of erosion and deposition, can produce the compensational-stacking patterns interpreted in the seismic-reflection data. Varying the time step impacted the heterogeneity of the model. Shorter time steps are characterized by less sediment accumulation, which results in less sediment diversion during the subsequent time step, more gradual migration of channel deposits, shorter offset distances of depocenters, and shorter length-scale heterogeneity compared to longer time steps. Thus, the controls on the compensational stacking and depocenter evolution are autogenic in these models. The processes and products of the slope fan of this study are broadly applicable to deep-water depositional systems in tectonically active slope basins. Future work will evaluate the influence of input variables and changing boundary conditions on heterogeneity of channel-and-lobe deposits of slope fans, as well as fluid flow behavior during hydrocarbon production.

ACKNOWLEDGMENTS

We thank the sponsors of the Quantitative Clastics Laboratory (http://www.beg.utexas.edu/qcl). We appreciate the donation of seismic-reflection data from ExxonMobil, Shell, and the Ministry of Energy and Energy Industries for Trinidad and Tobago to the University of Texas at Austin. We are grateful to Paradigm® for a generous donation of SeisEarth® interpretation and visualization software. We thank Lorena Moscardelli for invaluable discussions on project scope and the geology offshore Trinidad. We recognize Richard Sech, Morgan Sullivan, and Ashley Harris for inspiration to pursue an integrated subsurface characterization and forward stratigraphic modeling study. We thank two anonymous reviewers for recommendations that improved the clarity of this manuscript.

REFERENCES CITED

Adeogba, A. A., McHargue, T. R., & Graham, S. A. (2005). Transient fan architecture and depositional controls from near-surface 3-D seismic data, Niger Delta continental slope. AAPG bulletin, 89(5), 627-643.

Alzaga-Ruiz, H., Granjeon, D., Lopez, M., Seranne, M., & Roure, F. (2009). Gravitational collapse and Neogene sediment transfer across the western margin of the Gulf of Mexico: Insights from numerical models. Tectonophysics, 470(1), 21-41.

Armitage, D. A., Romans, B. W., Covault, J. A., & Graham, S. A. (2009). The influence of mass-transport-deposit surface topography on the evolution of turbidite architecture: The Sierra

Contreras, Tres Pasos Formation (Cretaceous), southern Chile. Journal of Sedimentary Research, 79(5), 287-301.

Avouac, J. P., & Burov, E. B. (1996). Erosion as a driving mechanism of intracontinental mountain growth. Journal of Geophysical Research: Solid Earth, 101(B8), 17747-17769.

Beaubouef, R. T., Abreu, V., & Van Wagoner, J. C. (2003, December). Basin 4 of the Brazos–Trinity slope system, western Gulf of Mexico: the terminal portion of a late Pleistocene lowstand systems tract. In Shelf margin deltas and linked down slope petroleum systems: Global significance and future exploration potential: Proceedings of the 23rd Annual Research Conference, Gulf Coast Section SEPM Foundation (pp. 45-66).

Beaubouef, R. T., & Friedmann, S. J. (2000, December). High resolution seismic/sequence stratigraphic framework for the evolution of Pleistocene intra slope basins, western Gulf of Mexico: depositional models and reservoir analogs. In Deep-water reservoirs of the world: Gulf Coast Section SEPM 20th Annual Research Conference (pp. 40-60).

Belderson, R. H., Kenyon, N. H., Stride, A. H., & Pelton, C. D. (1984). A 'braided'distributary system on the Orinoco deep-sea fan. Marine Geology, 56(1-4), 195-206.

Bouma, A. H., Normark, W. R., & Barnes, N. E. (1985). Submarine fans and related turbidite systems. SpringerVerlag Inc., Berlin and New York.

Brami, T. R., Pirmez, C., Archie, C., Heeralal, S., & Holman, K. L. (2000, December). Late Pleistocene deep-water stratigraphy and depositional processes, offshore Trinidad and Tobago. In Deep-water reservoirs of the world: Gulf Coast Section SEPM 20th Annual Research Conference (pp. 104-115).

Clift, P., & Gaedicke, C. (2002). Accelerated mass flux to the Arabian Sea during the middle to late Miocene. Geology, 30(3), 207-210.

Covault, J. A., & Romans, B. W. (2009). Growth patterns of deep-sea fans revisited: Turbidite-system morphology in confined basins, examples from the California Borderland. Marine Geology, 265(1), 51-66.

Covault, J. A., Romans, B. W., Fildani, A., McGann, M., & Graham, S. A. (2010). Rapid climatic signal propagation from source to sink in a southern California sediment-routing system. The Journal of Geology, 118(3), 247-259.

Covault, J. A., Romans, B. W., Graham, S. A., Fildani, A., & Hilley, G. E. (2011). Terrestrial source to deep-sea sink sediment budgets at high and low sea levels: Insights from tectonically active Southern California. Geology, 39(7), 619-622.

Damuth, J. E. (1994). Neogene gravity tectonics and depositional processes on the deep Niger Delta continental margin. Marine and Petroleum Geology, 11(3), 320-346.

Deptuck, M. E., Piper, D. J., Savoye, B., & Gervais, A. (2008). Dimensions and architecture of late Pleistocene submarine lobes off the northern margin of East Corsica. Sedimentology, 55(4), 869-898.

Deptuck, M. E., Sylvester, Z., & O'Byrne, C. (2012). Pleistocene seascape evolution above a "simple" stepped slope, western Niger Delta. Application of the principles of seismic geomorphology to continental slope and base-of-slope systems: Case studies from sea floor and near–sea floor analog: SEPM Special Publication, 99, 199-222.

de Gamero, M. L. D. (1996). The changing course of the Orinoco River during the Neogene: a review. Palaeogeography, Palaeoclimatology, Palaeoecology, 123(1-4), 385-402.

Dill, R. F., Dietz, R. S., & Stewart, H. (1954). Deep-sea channels and delta of the Monterey submarine canyon. Geological Society of America Bulletin, 65(2), 191-194.

Escalona, A., & Mann, P. (2011). Tectonics, basin subsidence mechanisms, and paleogeography of the Caribbean-South American plate boundary zone. Marine and Petroleum Geology, 28(1), 8-39.

Euzen, T., Joseph, P., Du Fornel, E., Lesur, S., Granjeon, D., & Guillocheau, F. (2004). Three-dimensional stratigraphic modelling of the Grès d'Annot system, Eocene-Oligocene, SE France. Geological Society, London, Special Publications, 221(1), 161-180.

Faugères, J. C., Gonthier, E., Griboulard, R., & Masse, L. (1993). Quaternary sandy deposits and canyons on the Venezuelan margin and south Barbados accretionary prism. Marine Geology, 110(1-2), 115-142.

Fernandez, R. L., Cantelli, A., Pirmez, C., Sequeiros, O., & Parker, G. (2014). Growth patterns of subaqueous depositional channel lobe systems developed over a basement with a downdip break in slope: Laboratory experiments. Journal of Sedimentary Research, 84(3), 168-182.

Fildani, A., McKay, M. P., Stockli, D., Clark, J., Dykstra, M. L., Stockli, L., & Hessler, A. M. (2016). The ancestral Mississippi drainage archived in the late Wisconsin Mississippi deep-sea fan. Geology, 44(6), 479-482.

Fildani, A., & Normark, W. R. (2004). Late Quaternary evolution of channel and lobe complexes of Monterey Fan. Marine Geology, 206(1), 199-223.

Flemings, P. B., & Jordan, T. E. (1989). A synthetic stratigraphic model of foreland basin development. Journal of Geophysical Research: Solid Earth, 94(B4), 3851-3866.

French, C. D., & Schenk, C. J. (2004). Map Showing Geology, Oil and Gas Fields, and Geologic Provinces of the Caribbean Region, Open File Report 97-470-K. US Geological Survey, Denver, CO, https://pubs.usgs.gov/of/1997/ofr-97-470/OF97-470K/index.html.

Garciacaro, E., Mann, P., & Escalona, A. (2011a). Regional structure and tectonic history of the obliquely colliding Columbus foreland basin, offshore Trinidad and Venezuela. Marine and Petroleum Geology, 28(1), 126-148.

Garciacaro, E., Escalona, A., Mann, P., Wood, L., Moscardelli, L., & Sullivan, S. (2011b). Structural controls on Quaternary deepwater sedimentation, mud diapirism, and hydrocarbon distribution within the actively evolving Columbus foreland basin, eastern offshore Trinidad. Marine and Petroleum Geology, 28(1), 149-176.

Glenton, P. N., Sutton, J. T., McPherson, J. G., Fittall, M. E., Moore, M. A., Heavysege, R. G., & Box, D. (2013, March). Hierarchical approach to facies and property distribution in a basin-floor fan model, Scarborough Gas Field, North West Shelf, Australia. In IPTC 2013: International Petroleum Technology Conference.

Granjeon, D. (1997). Modélisation stratigraphique déterministe: conception et applications d'un modéle diffusif 3 D multilithologique. PhD dissertation, Université de Rennes.

Granjeon, D. (2014). 3D forward modelling of the impact of sediment transport and base level cycles on continental margins and incised valleys. Depositional Systems to Sedimentary Successions on the Norwegian Continental Margin: International Association of Sedimentologists, Special Publication, 46, 453-472.

Granjeon, D., & Joseph, P. (1999). Concepts and applications of a 3-D multiple lithology, diffusive model in stratigraphic modeling. Numerical experiments in stratigraphy: Recent advances in stratigraphic and sedimentologic compouter simulations: SEPM Special Publication, 62, 197-210.

Gvirtzman, Z., Csato, I., & Granjeon, D. (2014). Constraining sediment transport to deep marine basins through submarine channels: The Levant margin in the Late Cenozoic. Marine Geology, 347, 12-26.

Hamilton, P. B., Strom, K. B., & Hoyal, D. C. (2015). Hydraulic and sediment transport properties of autogenic avulsion cycles on submarine fans with supercritical distributaries. Journal of Geophysical Research: Earth Surface, 120(7), 1369-1389.

Harris, A. D., Covault, J. A., Madof, A. S., Sun, T., Sylvester, Z., & Granjeon, D. (2016). Three-Dimensional Numerical Modeling of Eustatic Control On Continental-Margin Sand Distribution. Journal of Sedimentary Research, 86(12), 1434-1443.

Hawie, N., Deschamps, R., Granjeon, D., Nader, F. H., Gorini, C., Müller, C., ... & Baudin, F. (2017). Multi-scale constraints of sediment source to sink systems in frontier basins: a forward stratigraphic modelling case study of the Levant region. Basin Research, 29(S1), 418-445.

Heezen, B. C., Tharp, M., & Ewing, M. (1959). The floors of the oceans I. The North Atlantic. Geological Society of America Special Papers, 65, 1-126.

Hoyal, D. C. H., Demko, T., Postma, G., Wellner, R. W., Pederson, K., Abreu, V., ... & Strom, K. (2014). Evolution, architecture and stratigraphy of Froude supercritical submarine fans. In American Association of Petroleum Geologists Annual Convention and Exhibition, April (pp. 6-9).

Hoyal, D., Sheets, B., Wellner, R., Box, D., Sprague, A., & Bloch, R. (2011). Architecture of Froude critical-supercritical submarine fans: tank experiments versus field observations. In American Association of Petroleum Geologists Annual Convention and Exhibition, April (pp. 10-13).

Huyghe, P., Foata, M., Deville, E., Mascle, G., & Caramba Working Group. (2004). Channel profiles through the active thrust front of the southern Barbados prism. Geology, 32(5), 429-432.

Jobe, Z. R., Sylvester, Z., Howes, N., Pirmez, C., Parker, A., Cantelli, A., ... & Prather, B. (2017). High-resolution, millennial-scale patterns of bed compensation on a sand-rich intraslope submarine fan, western Niger Delta slope. Geological Society of America Bulletin, 129(1-2), 23-37.

Kneller, B., Dykstra, M., Fairweather, L., & Milana, J. P. (2016). Mass-transport and slope accommodation: implications for turbidite sandstone reservoirs. AAPG Bulletin, 100(2), 213-235.

Lake, L. W., & Jensen, J. L. (1989). A review of heterogeneity measures used in reservoir characterization. Society of Petroleum Engineers.

Leonard, R. (1983). Geology and hydrocarbon accumulations, Columbus Basin, offshore Trinidad. AAPG Bulletin, 67(7), 1081-1093.

Maier, K. L., Fildani, A., Paull, C. K., Graham, S. A., McHargue, T. R., Caress, D. W., & McGann, M. (2011). The elusive character of discontinuous deep-water channels: New insights from Lucia Chica channel system, offshore California. Geology, 39(4), 327-330.

Maier, K. L., Fildani, A., McHargue, T. R., Paull, C. K., Graham, S. A., & Caress, D. W. (2012). Punctuated deep-water channel migration: high-resolution subsurface data from the Lucia Chica channel system, Offshore California, USA. Journal of Sedimentary Research, 82(1), 1-8.

McHargue, T., Pyrcz, M. J., Sullivan, M. D., Clark, J. D., Fildani, A., Romans, B. W., ... & Drinkwater, N. J. (2011). Architecture of turbidite channel systems on the continental slope: patterns and predictions. Marine and Petroleum Geology, 28(3), 728-743.

Menard Jr, H. W. (1955). Deep-sea channels, topography, and sedimentation. AAPG Bulletin, 39(2), 236-255.

Miller, J. K., Sun, T., Li, H., Stewart, J., Genty, C., Li, D., & Lyttle, C. (2008, January). Direct modeling of reservoirs through forward process-based models: Can we get there?. In International petroleum technology conference. International Petroleum Technology Conference.

Milliman, J. D., & Farnsworth, K. L. (2013). River discharge to the coastal ocean: a global synthesis. Cambridge University Press.

Mitchum Jr, R. M., Vail, P. R., & Sangree, J. B. (1977). Seismic stratigraphy and global changes of sea level: Part 6. Stratigraphic interpretation of seismic reflection patterns in depositional sequences: Section 2. Application of seismic reflection configuration to stratigraphic interpretation. AAPG Memoir, 26, 117-133.

Mize, K. L. (2004). Controls on the morphology and development of deep-marine channels, Eastern Offshore Trinidad and Venezuela. MS dissertation, The University of Texas at Austin.

Moscardelli, L. G. (2007). Mass transport processes and deposits in offshore Trinidad and Venezuela, and their role in continental margin development. PhD dissertation, The University of Texas at Austin.

Moscardelli, L., & Wood, L. (2008). New classification system for mass transport complexes in offshore Trinidad. Basin research, 20(1), 73-98.

Moscardelli, L., Wood, L., & Mann, P. (2006). Mass-transport complexes and associated processes in the offshore area of Trinidad and Venezuela. AAPG bulletin, 90(7), 1059-1088.

Moscardelli, L., Wood, L. J., & Dunlap, D. B. (2012). Shelf-edge deltas along structurally complex margins: a case study from eastern offshore Trinidad. AAPG bulletin, 96(8), 1483-1522.

Mutti, E., & Normark, W. R. (1987). Comparing examples of modern and ancient turbidite systems: problems and concepts. In Marine clastic sedimentology (pp. 1-38). Springer Netherlands.

Mutti, E., & Normark, W. R. (1991). An integrated approach to the study of turbidite systems. In Seismic facies and sedimentary processes of submarine fans and turbidite systems (pp. 75-106). Springer New York.

Normark, W. R., Posamentier, H., & Mutti, E. (1993). Turbidite systems: state of the art and future directions. Reviews of Geophysics, 31(2), 91-116.

Patterson, M. B., Blom, F., Griffith, C. M., Tepper, B. J., & Truempy, D. (2001). Sweet Music in the Columbus Basin: From Mozart to Haydn, and Then? In American Association of Petroleum Geologists Annual Convention and Exhibition, June.

Pettingill, H. S., & Weimer, P. (2002). Worlwide deepwater exploration and production: Past, present, and future. The Leading Edge, 21(4), 371-376.

Piper, D. J., & Normark, W. R. (2001). Sandy fans--from Amazon to Hueneme and beyond. AAPG bulletin, 85(8), 1407-1438.

Pinheiro-Moreira, J. L. (2000). Stratigraphie sismique et modélisation stratigraphique des dépôts de l'Éocène du Bassin de Santos (marge brésilienne). PhD dissertation, Université de Rennes.

Pirmez, C., Beaubouef, R. T., Friedmann, S. J., & Mohrig, D. C. (2000, December). Equilibrium profile and baselevel in submarine channels: examples from Late Pleistocene systems and implications for the architecture of deepwater reservoirs. In Global deep-water reservoirs: Gulf Coast Section SEPM Foundation 20th Annual Bob F. Perkins Research Conference (pp. 782-805).

Postma, G., Hoyal, D. C., Abreu, V., Cartigny, M. J., Demko, T., Fedele, J. J., ... & Pederson, K. H. (2016). Morphodynamics of supercritical turbidity currents in the channel-lobe transition zone. In Submarine Mass Movements and their Consequences (pp. 469-478). Springer International Publishing.

Prather, B. E. (2003). Controls on reservoir distribution, architecture and stratigraphic trapping in slope settings. Marine and Petroleum Geology, 20(6), 529-545.

Prather, B. E., Pirmez, C., & Winker, C. D. (2012). Stratigraphy of linked intraslope basins: Brazos-Trinity system western Gulf of Mexico. Application of the Principles of Seismic Geomorphology to Continental-Slope and Base-of-Slope Systems: Case Studies from Seafloor and Near-Seafloor Analogues: SEPM, Special Publication, 99, 83-110.

Prélat, A., Covault, J. A., Hodgson, D. M., Fildani, A., & Flint, S. S. (2010). Intrinsic controls on the range of volumes, morphologies, and dimensions of submarine lobes. Sedimentary Geology, 232(1), 66-76.

Prélat, A., Hodgson, D. M., & Flint, S. S. (2009). Evolution, architecture and hierarchy of distributary deep-water deposits: a high-resolution outcrop investigation from the Permian Karoo Basin, South Africa. Sedimentology, 56(7), 2132-2154.

Pyrcz, M. J., & Deutsch, C. V. (2014). Geostatistical reservoir modeling. Oxford university press.

Pyrcz, M. J., Sech, R. P., Covault, J. A., Willis, B. J., Sylvester, Z., & Sun, T. (2015). Stratigraphic rule-based reservoir modeling. Bulletin of Canadian Petroleum Geology, 63(4), 287-303.

Rabineau, M., Berné, S., Aslanian, D., Olivet, J. L., Joseph, P., Guillocheau, F., ... & Granjeon, D. (2005). Sedimentary sequences in the Gulf of Lion: a record of 100,000 years climatic cycles. Marine and Petroleum Geology, 22(6), 775-804.

Richards, M., Bowman, M., & Reading, H. (1998). Submarine-fan systems I: characterization and stratigraphic prediction. Marine and Petroleum Geology, 15(7), 689-717.

Rowan, M. G., Peel, F. J., & Vendeville, B. C. (2004). Gravity-driven fold belts on passive margins. AAPG Memoir, 82, 157-182.

Ryan, W. B., Carbotte, S. M., Coplan, J. O., O'Hara, S., Melkonian, A., Arko, R., ... & Bonczkowski, J. (2009). Global multi-resolution topography synthesis. Geochemistry, Geophysics, Geosystems, 10(3).

Shepard, F. P. & Emery, K. O. (1941). Submarine topography off the California coast: Canyon and tectonic interpretation. Geological Society of America Special Papers, 31, 1-171.

Sømme, T. O., Helland-Hansen, W., & Granjeon, D. (2009). Impact of eustatic amplitude variations on shelf morphology, sediment dispersal, and sequence stratigraphic interpretation: Icehouse versus greenhouse systems. Geology, 37(7), 587-590.

Spinewine, B., Sequeiros, O. E., Garcia, M. H., Beaubouef, R. T., Sun, T., Savoye, B., & Parker, G. (2009). Experiments on wedge-shaped deep sea sedimentary deposits in minibasins and/or on channel levees emplaced by turbidity currents. Part II. Morphodynamic evolution of the wedge and of the associated bedforms. Journal of Sedimentary Research, 79(8), 608-628.

Sullivan, S. M. (2005). Geochemistry, sedimentology, and morphology of mud volcanoes, eastern offshore Trinidad. MS dissertation, The University of Texas at Austin.

Sullivan, M. D., Foreman, J. L., Jennette, D. C., Stern, D., Jensen, G. N., & Goulding, F. J. (2004a). An integrated approach to characterization and modeling of deep-water reservoirs, Diana field, western Gulf of Mexico. AAPG Memoir, 80, 215-234.

Sullivan, M., Jensen, G., Goulding, F., Jennette, D., Foreman, L., & Stern, D. (2000, December). Architectural analysis of deep-water outcrops: Implications for exploration and development of the Diana sub-basin, western Gulf of Mexico. In Deep-water reservoirs of the world: Gulf Coast Section SEPM Foundation 20th Annual Research Conference (pp. 1010-1032).

Sullivan, S., Wood, L. J., & Mann, P. (2004b, December). Distribution, nature and origin of mobile mud features offshore Trinidad. In Salt-sediment interactions and hydrocarbon prospectivity: Concepts, applications, and case studies for the 21st century: Gulf Coast Section SEPM 24th Annual Research Conference (pp. 840-867).

Sun, T., Ghayour, K., Hall, B., & Miller, J. (2010, December). Process-based modeling of deep water depositional systems. In Seismic Imaging of Depositional and Geomorphic Systems: Gulf Coast Section SEPM Foundation 30th Annual Bob F. Perkins Research Conference (pp. 88-112).

Sutton, J. T., Glenton, P. N., Fittall, M. E., Moore, M. A., & Box, D. (2013, March). Reservoir Simulation to Investigate the Effect of Flow Baffles in a Basin-Floor Fan, Scarborough Field, North West Shelf, Australia. In SPE Middle East Oil and Gas Show and Conference. Society of Petroleum Engineers.

Sydow, J., Finneran, J., Bowman, A. P., Rosen, H., Fillon, R., & Anderson, J. (2003, December). Stacked shelf-edge delta reservoirs of the Columbus Basin, Trinidad, West Indies. In Shelf margin deltas and linked down slope petroleum systems: Global significance and future exploration potential: Proceedings of the 23rd Annual Research Conference, Gulf Coast Section SEPM Foundation (pp. 441-465).

Sylvester, Z., Deptuck, M. E., Prather, B. E., Pirmez, C., & O'Byrne, C. (2012). Seismic stratigraphy of a shelf-edge delta and linked submarine channels in the northeastern Gulf of Mexico. Application of the Principles of Seismic Geomorphology to Continental-Slope and Base-of-Slope Systems: Case Studies from Seafloor and Near-Seafloor Analogues: SEPM, Special Publication, 99, 31-59.

Tucker, G. E., & Slingerland, R. L. (1994). Erosional dynamics, flexural isostasy, and long-lived escarpments: A numerical modeling study. Journal of Geophysical Research: Solid Earth, 99(B6), 12229-12243.

Walker, R. G. (1992). Turbidites and submarine fans. Facies models response to sea-level changes, 239-263.

Warne, A. G., Meade, R. H., White, W. A., Guevara, E. H., Gibeaut, J., Smyth, R. C., ... & Tremblay, T. (2002). Regional controls on geomorphology, hydrology, and ecosystem integrity in the Orinoco Delta, Venezuela. Geomorphology, 44(3), 273-307.

Weber, J. C., Dixon, T. H., DeMets, C., Ambeh, W. B., Jansma, P., Mattioli, G., ... & Pérez, O. (2001). GPS estimate of relative motion between the Caribbean and South American plates, and geologic implications for Trinidad and Venezuela. Geology, 29(1), 75-78.

Willgoose, G., Bras, R. L., & Rodriguez-Iturbe, I. (1991). A coupled channel network growth and hillslope evolution model: 1. Theory. Water Resources Research, 27(7), 1671-1684.

Wood, L. J. (2000). Chronostratigraphy and tectonostratigraphy of the Columbus Basin, eastern offshore Trinidad. AAPG bulletin, 84(12), 1905-1928.

Wood, L. J., & Mize-Spansky, K. L. (2009). Quantitative seismic geomorphology of a Quaternary leveed-channel system, offshore eastern Trinidad and Tobago, northeastern South America. AAPG Bulletin, 93(1), 101-125.

Wood, L. J., & Roberts, C. (2001). Opportunity in a world-class hydrocarbon basin: Trinidad and Tobago's eastern offshore marine province. Houston Geological Society Bulletin, 43(10), 37-43, 45.

FIGURE CAPTIONS

Figure 1. Example of Brazos-Trinity Basin II slope-fan depositional architecture. a. Co-rendered bathymetry and slope of Basin II from the BOEM Northern Gulf of Mexico Deepwater Bathymetry Grid from 3D Seismic (https://www.boem.gov/Gulf-of-Mexico-Deepwater-Bathymetry/). b. Isochron map of the Upper Sequence. c. Upper Sequence stratigraphic architecture. d. Isochron maps of mass-transport complex, distributary channel-lobe complex, and leveed-channel complex of the Upper Sequence. Parts b-d modified from Beaubouef and Friedmann (2000).

Figure 2. Caribbean geologic setting. Bathymetry is from Geomapapp.org (Ryan et al., 2009). Faults are black lines (French and Schenk, 2004).

Figure 3. a. Co-rendered bathymetry and slope offshore Trinidad. Modified from Mize (2004), Sullivan et al. (2004b), Sullivan (2005), Moscardelli and Wood (2008), and Wood and Mize-Spansky (2009). b. Proportional slice of seismic-reflection amplitude between horizons ‘c’ and ‘f’ (see Figure 4 for locations of horizons ‘c’ and ‘f’).

Figure 4. a. Time-structure maps of horizons ‘c’ and ‘f.’ Horizon ‘c’ is the initial bathymetry of the stratigraphic forward model. Horizon ‘f’ is the seafloor. b-d. Seismic-reflection profiles of the shallowest depositional sequence in block 25A. Uninterpreted (top) and interpreted (bottom) profiles. Horizons ‘a’-‘f’ are red. Modified from Moscardelli et al. (2006) and Garciacaro et al. (2011).

Figure 5. Isochron maps of the shallowest depositional sequence in block 25A. Line-drawing trace of horizons ‘a’-‘f’ is from Figure 4 part d. Mass-transport complexes are between horizons ‘a’ and ‘b.’ A submarine fan comprising channel and lobe deposits is between horizons ‘c’ and ‘f’. Modified from Moscardelli et al. (2006) and Garciacaro et al. (2011).

Figure 6. Reference-case model (10 kyr time step). a. Isochore map of the entire model. b. Sand percentage map, calculated based on the proportion of coarse- and medium-grained sand. c. Difference between the thickness of the model and the thickness of the depositional sequence in block 25A, assuming a sound velocity of 2000 m/s. d. Grain-size distribution at 0.104, 0.064, and 0.034 time steps. e. Isochore maps of depositional sequences within the model showing major phases of sediment diversion. f. Cross sections of the model. Left (L) and right (R) orientations in cross sections are left and right in maps in parts a-e. Locations shown in part d. See Supplementary Files 1-2 for the detailed stratigraphic evolution.

Figure 7. Isochore and sand percentage maps and cross sections of the 20 kyr time-step model (a), the 5 kyr time-step model (b), and the 1 kyr time-step model (c). Left (L) and right (R) orientations in cross sections are left and right in maps. Cross-section locations shown in part a. See Supplementary Files 3-8 for the detailed stratigraphic evolution.

Figure 8. Sand percentage map of reference-case model (10 kyr time step) of the sequence deposited between 0.074-0.064 Ma (a-b) compared to the object-based model of the A-50 reservoir of the Diana field, Gulf of Mexico deep-water slope (c). In part c, net-to-gross ranges from > 0.95 in the proximal area (red) to <0.40 in the distal area (purple). Part c modified from Sullivan et al. (2004a).

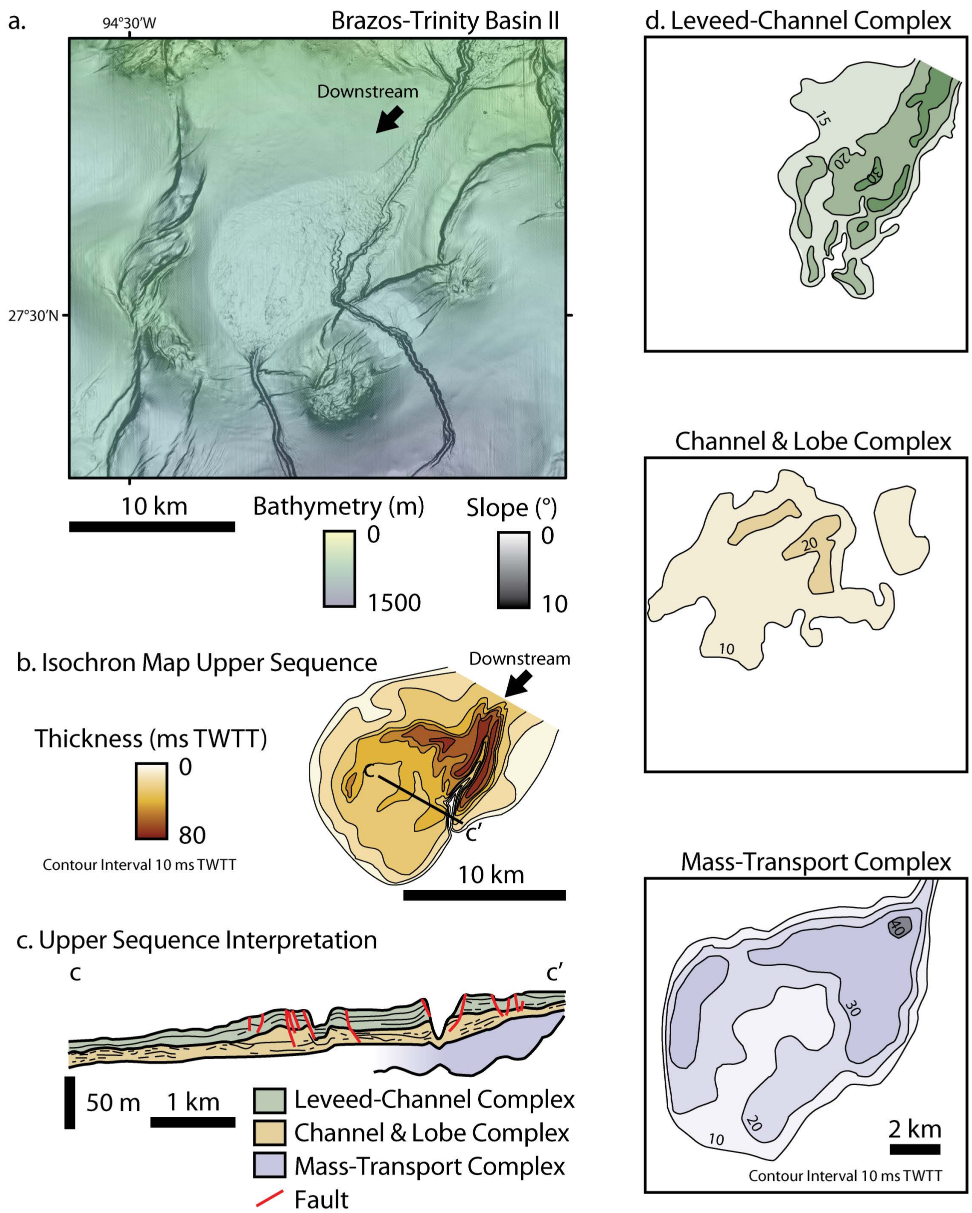

a.
94°30'W
Brazos-Trinity Basin II
Downstream
27°30'N
10 km
Bathymetry (m)
0
1500
Slope (°)
0
10
b. Isochron Map Upper Sequence
Downstream
Thickness (ms TWTT)
0
80
Contour Interval 10 ms TWTT
c
c'
10 km
c. Upper Sequence Interpretation
c
c'
50 m
1 km
Leveed-Channel Complex
Channel & Lobe Complex
Mass-Transport Complex
Fault
d. Leveed-Channel Complex
15
20
30
Channel & Lobe Complex
20
10
Mass-Transport Complex
40
30
20
10
2 km
Contour Interval 10 ms TWTT

Figure 1

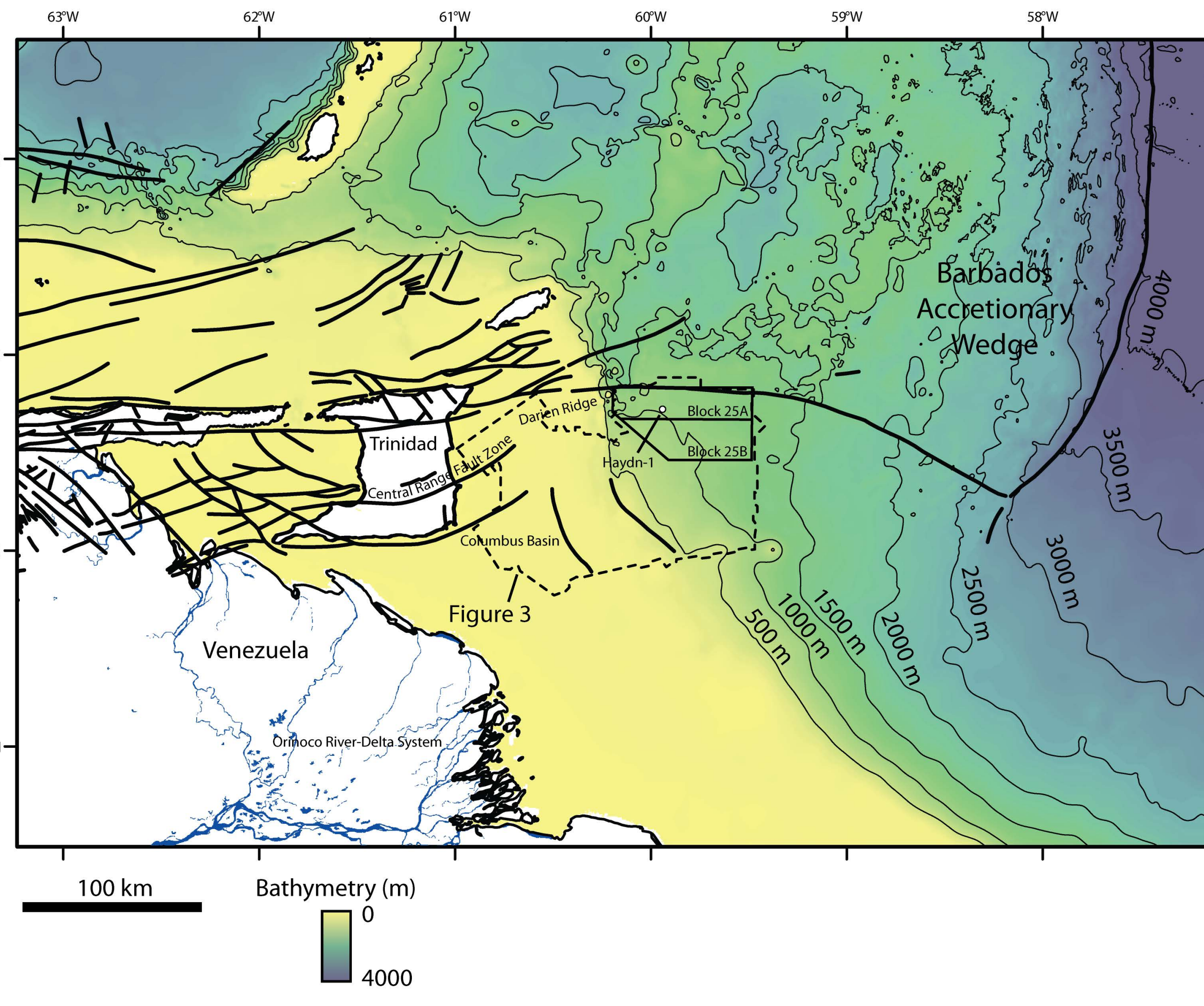

63°W
62°W
61°W
60°W
59°W
58°W
12°N
11°N
10°N
9°N
Barbados
Accretionary
Wedge
Trinidad
Darien Ridge
Central Range Fault Zone
Block 25A
Block 25B
Haydn-1
Columbus Basin
Figure 3
Venezuela
Orinoco River-Delta System
500 m
1000 m
1500 m
2000 m
2500 m
3000 m
3500 m
4000 m
100 km
Bathymetry (m)
0
4000

Figure 2

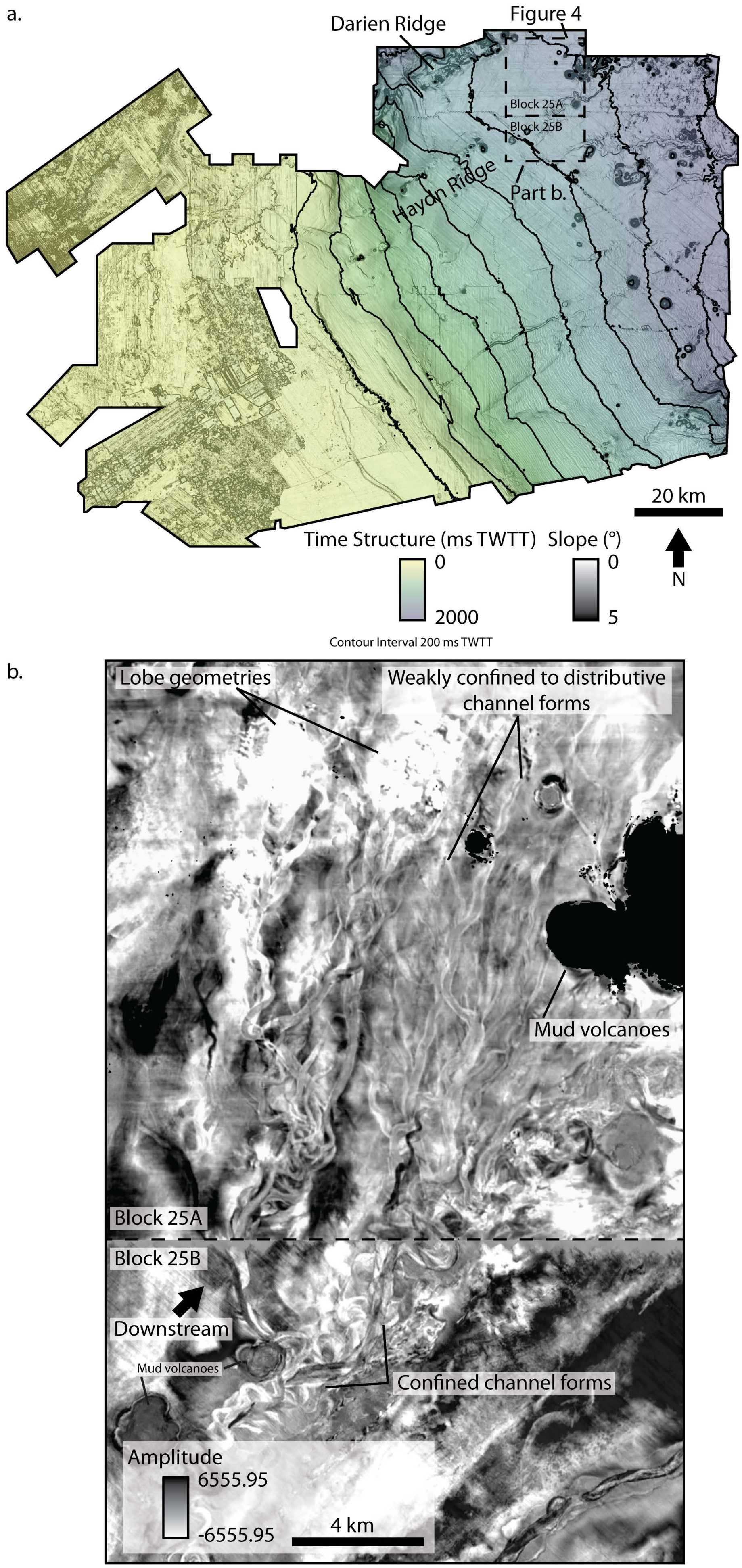
a.
Darien Ridge
Figure 4
Block 25A
Block 25B
Haydn Ridge
Part b.
20 km
N
Time Structure (ms TWTT)
0
2000
Slope (°)
0
5
Contour Interval 200 ms TWTT
b.
Lobe geometries
Weakly confined to distributive channel forms
Mud volcanoes
Block 25A
Block 25B
Downstream
Mud volcanoes
Confined channel forms
Amplitude
6555.95
-6555.95
4 km

Figure 3

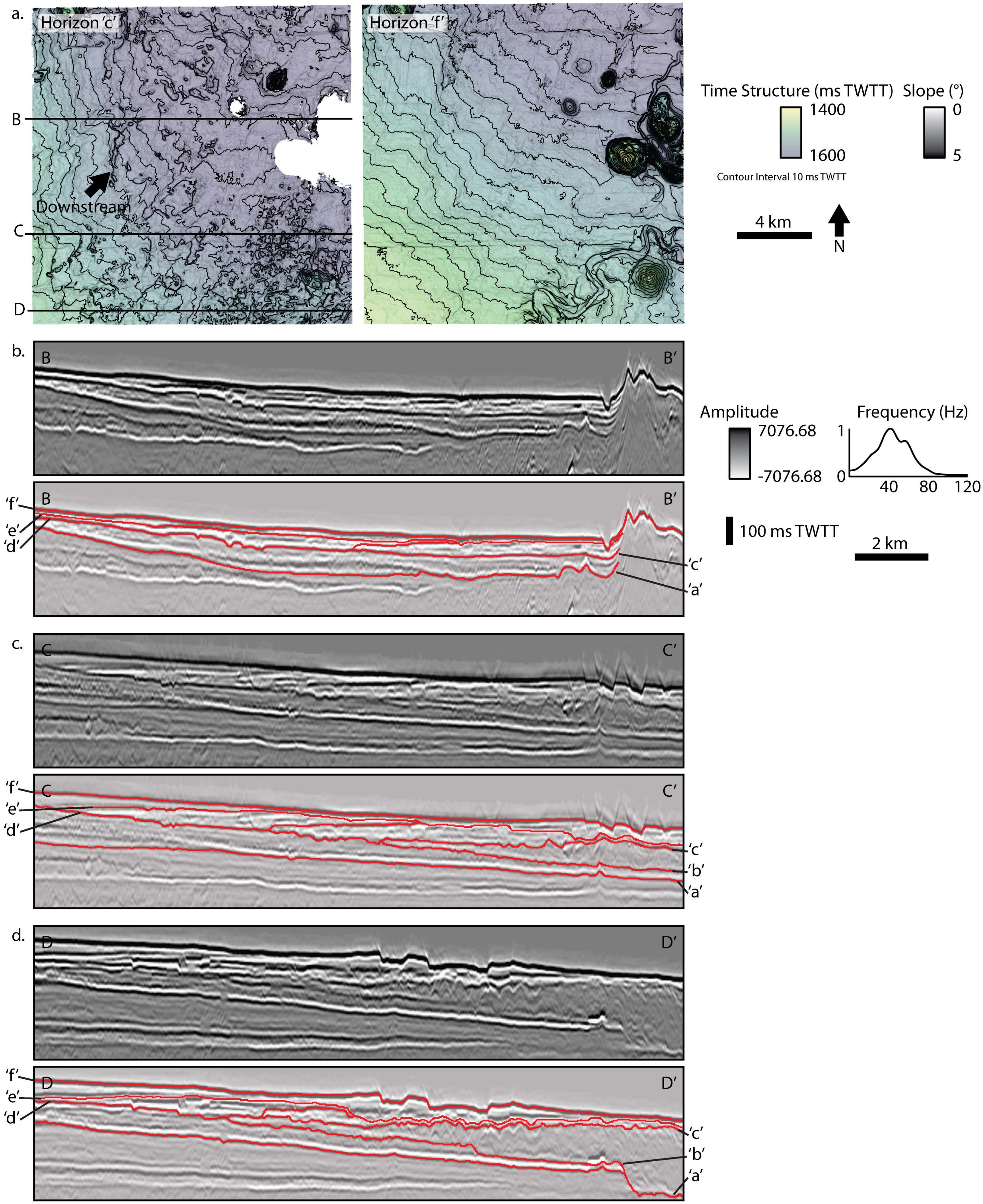
a.
Horizon 'c'
Horizon 'f'
B
C
D
Downstream
Time Structure (ms TWTT)
1400
1600
Contour Interval 10 ms TWTT
Slope (°)
0
5
4 km
N
b.
B
B'
'f'
'e'
'd'
'c'
'a'
Amplitude
7076.68
-7076.68
Frequency (Hz)
1
0
40
80
120
100 ms TWTT
2 km
c.
C
C'
'b'
d.
D
D'

Figure 4

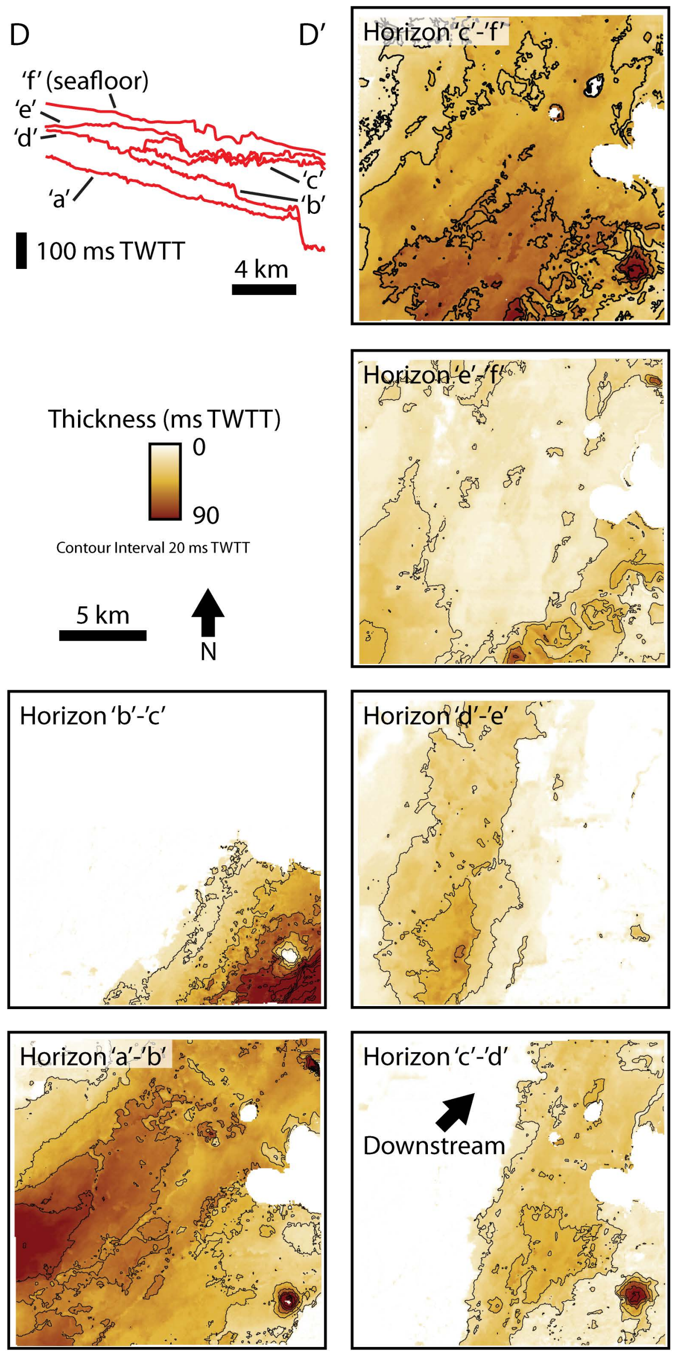

D
D′
'f' (seafloor)
'e'
'd'
'c'
'b'
'a'
100 ms TWTT
4 km
Horizon 'c'-'f'
Horizon 'e'-'f'
Thickness (ms TWTT)
0
90
Contour Interval 20 ms TWTT
5 km
N
Horizon 'b'-'c'
Horizon 'd'-'e'
Horizon 'a'-'b'
Horizon 'c'-'d'
Downstream

Figure 5

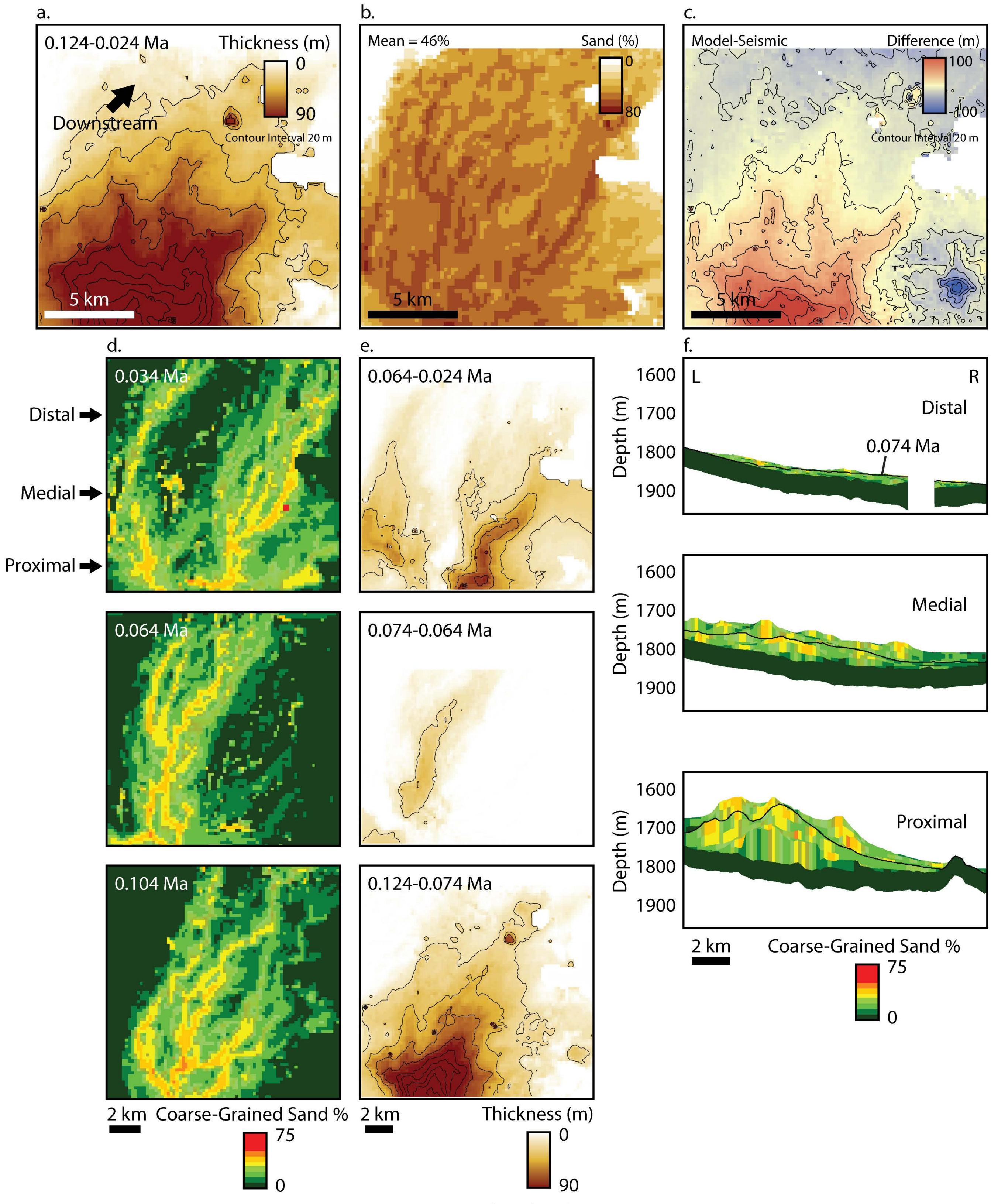

a.
0.124-0.024 Ma
Thickness (m)
0
90
Downstream
Contour Interval 20 m
5 km
b.
Mean = 46%
Sand (%)
0
80
5 km
c.
Model-Seismic
Difference (m)
100
-100
Contour Interval 20 m
5 km
d.
0.034 Ma
Distal
Medial
Proximal
0.064 Ma
0.104 Ma
2 km
Coarse-Grained Sand %
75
0
e.
0.064-0.024 Ma
0.074-0.064 Ma
0.124-0.074 Ma
2 km
Thickness (m)
0
90
Contour Interval 20 m
f.
L
R
Distal
0.074 Ma
Medial
Proximal
Depth (m)
1600
1700
1800
1900
2 km
Coarse-Grained Sand %
75
0

Figure 6

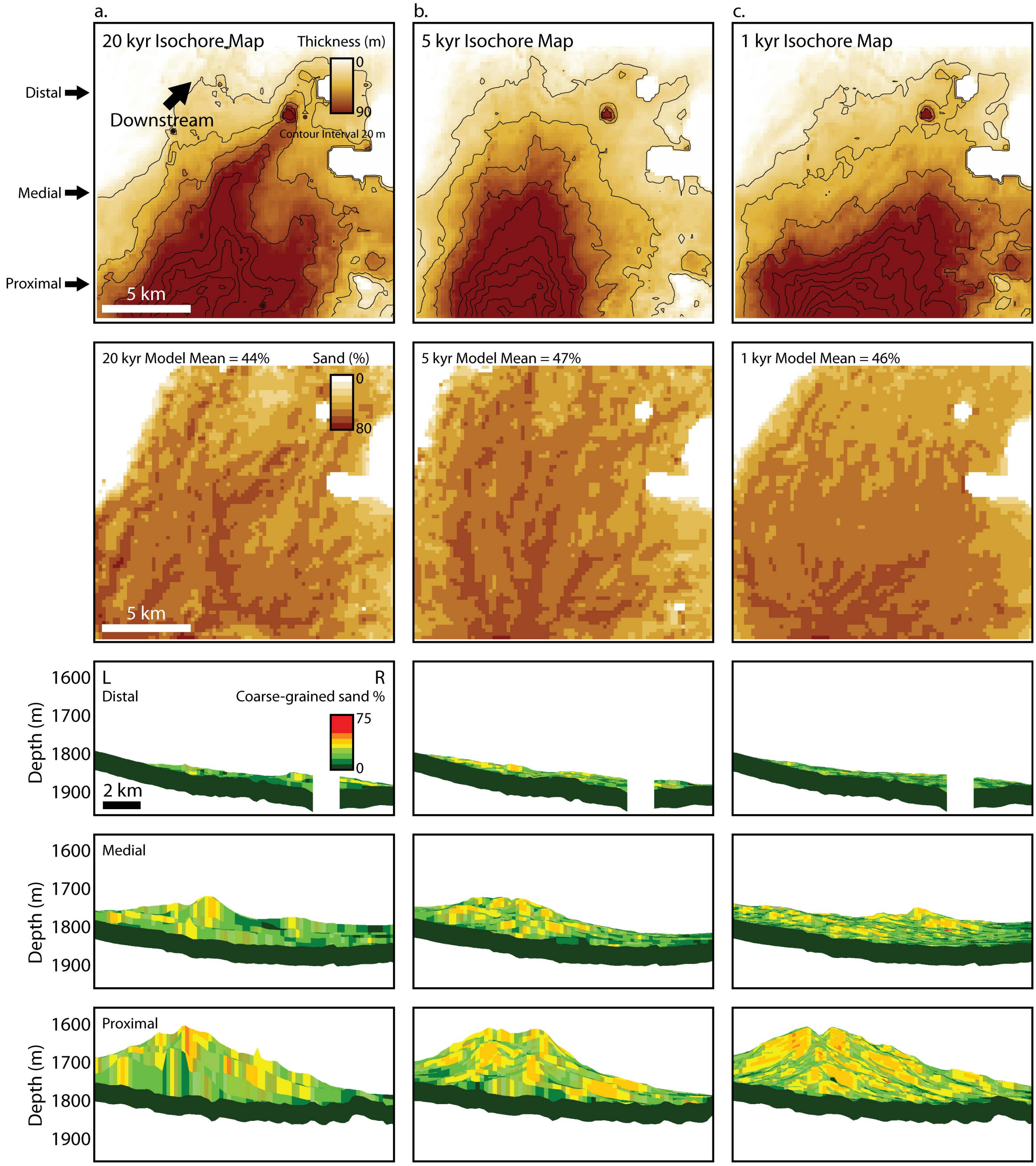

a.
b.
c.
20 kyr Isochore Map
Thickness (m)
0
90
Contour Interval 20 m
Downstream
Distal
Medial
Proximal
5 km
5 kyr Isochore Map
1 kyr Isochore Map
20 kyr Model Mean = 44%
Sand (%)
0
80
5 km
5 kyr Model Mean = 47%
1 kyr Model Mean = 46%
L
R
Distal
Coarse-grained sand %
75
0
2 km
Depth (m)
1600
1700
1800
1900
Medial
Proximal

Figure 7

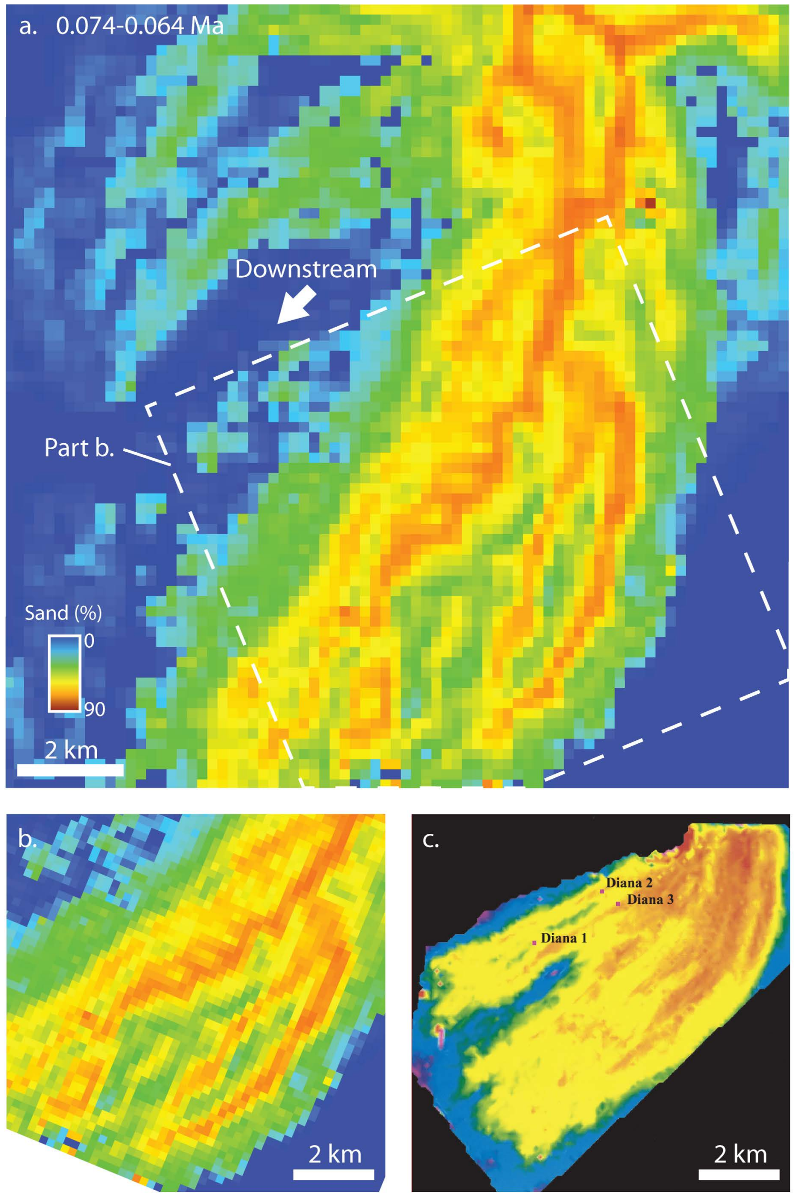
a. 0.074-0.064 Ma
Downstream
Part b.
Sand (%)
0
90
2 km
b.
2 km
c.
Diana 2
Diana 3
Diana 1
2 km

Figure 8

Table 1. Model Input Parameters

Area: 17 km x 17 km

Cell size: 200 m x 200 m

Duration: 124.5-24.5 ka

Time steps: 10 kyr reference case, 20 kyr, 5 kyr, 1 kyr

Sediment load: 230 km^3/Ma

Grain-size classes: 20% coarse sand (0.5 mm), 30% medium sand (0.3 mm), 40% fine sand (0.125 mm), 10% silt/clay (0.004 mm)

Water discharge: 100 m^3/s

K_w: 10 (coarse sand), 20 (medium sand), 40 (fine sand), 100 (silt/clay)

K_s: 0.009 (coarse sand), 0.007 (medium sand), 0.005 (fine sand), 0.001 (silt/clay)